BULLETIN OF THE
GREEK MATHEMATICAL SOCIETY
Volume 54, 2007 (167–178)

A Wavelet-Galerkin technique for the Wave-Current-Seabed Interaction Problem in Variable Bathymetry Regions

Th.P. Gerostathis, K.S. Politis, K.A. Belibassakis and G.A. Athanassoulis

Received 31 December 2006 Accepted 7 September 2007

Abstract

A Wavelet-Galerkin technique is developed and applied to the wave-current-seabed interaction problem, with application to wave scattering by steady currents in variable bathymetry regions. We consider obliquely incident waves on a horizontally non-homogeneous current in a variable-depth strip, which is characterized by straight and parallel depth-contours. The flow associated with the current is assumed to be parallel to the isobaths and it is considered to be known. In a finite subregion containing the bottom irregularity the horizontal current has a general structure. Outside this region, the current is assumed to be uniform (or zero). The present method is based on an equivalent reformulation of the wave-current-seabed scattering problem as a coupled-mode system of horizontal equations, obtained by Belibassakis & Athanassoulis, [1] using a variational principle and a rapidly-convergent local-mode series expansion of the wave field. In this work, a wavelet representation of the horizontal modal amplitudes is introduced. The latter, in conjunction with a Galerkin formulation, leads to an algebraic system of equations for the corresponding wavelet coefficients. The main advantage of the present Wavelet-Galerkin method, in comparison with other numerical techniques (e.g. finite differences, FEM etc), is their intrinsic ability to simultaneously resolve the variety of spatial scales, that are present in each modal amplitude, leading finally to a robust and computationally efficient numerical scheme. The present approach can be considered as an extension of the works by Belibassakis & Athanassoulis [1], Belibassakis [2] and Smith [3], [4], and some of its main features are that it can be further elaborated to treat lateral discontinuities (e.g. vertical vortex sheets) and more general vertical current profiles with cross-jet component, and to include the effects of weak nonlinearity.

Keywords: water waves, currents, wavelets

1. Introduction

The characteristics of surface gravity waves can be strongly affected as they propagate through non-homogeneous currents and/or depth inhomogeneities that occur in variable bathymetry regions. For example, in cases of obliquely propagating waves through opposing currents, large amplitude waves can be produced see, e.g., [5], escalating to freak waves when enhanced by inshore effects due to sloping seabeds, see, e.g., [6], [7], [8].

In this work we consider the problem of scattering of obliquely incident waves on a horizontally non-homogeneous steady current, in a variable-bathymetry region characterised by straight and parallel bottom contours. The current flow is taken to be parallel to the bottom contours and is given. The horizontal current profile is assumed to be general in a finite subregion, e.g. monotonic or periodic with characteristic width ℓ and uniform (or negligible) outside this region. Moreover, we assume that the current varies slowly, i.e. changes in the current velocity occur over length scales much longer than the characteristic wave length, and that the wave flow is irrotational (at first order approximation). Restricting ourselves to linear, monochromatic waves, periodic in the $y-$direction, the wave potential, including the scattering effect by the current, can be obtained as a solution to the modified Helmholtz equation, subject to appropriate boundary conditions.

The above problem is treated by the development of a Wavelet-Galerkin technique applied to an equivalent reformulation in the form of a coupled-mode system of horizontal equations, as is obtained in [1], using a variational principle and a rapidly converged local series expansion of the wave potential. The technique is based on a wavelet series representation for the horizontal modal amplitudes of the local series. This representation, in conjunction with a Galerkin formulation, leads to an algebraic system of equations for the corresponding wavelet coefficients. Wavelet-Galerkin technique is preferred to other (e.g. FD, FEM etc), due to wavelets intrinsic ability to simultaneously resolve the variety of spatial scales, that are present in each modal amplitude, leading finally to a robust and computationally efficient numerical scheme. Also, using wavelets of increasing smoothness, a small number of grid points per wavelength is required for a numerically accurate and stable computation see e.g. [9]. Furthermore, the system of equations may be solved adaptively, see, e.g. [10], leading to computationally economical solutions.

In order to illustrate the effects of the structure of the current and of the bottom slope on the wave characteristics, numerical results are presented and discussed in the case of waves propagating through a monotonic current in variable depth strips.

2. Differential formulation of the problem

Following the formulation presented in [1], we consider the propagation of surface waves along a channel according to linear theory. It is assumed that the bottom is rigid

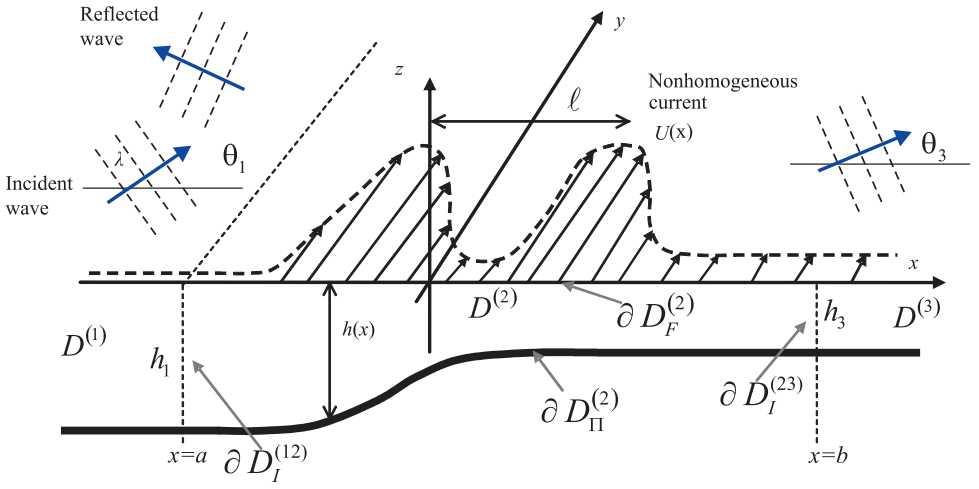

Figure 1: Geometrical configuration and basic notation

and its surface is characterised by straight and parallel bottom contours lying between two regions of constant but possibly different depth, h_1 (region of incidence) and h_2 (region of transmission); see Fig. 1. A Cartesian coordinate system is introduced, with its origin at some point on the mean water level (in the variable bathymetry region), the z-axis is taken vertically upwards and the y-axis being directed parallel to the bottom contours. The function $h(x) \in C^2(I\!R)$ represents the local depth, measured from the mean water level, and is such that: $h(x) = h(\alpha) = h_1$, for all $x \leq \alpha$ and $h(x) = h(\beta) = h_1$, for all $x \geq \beta$. The fluid domain is decomposed in three subdomains $D^{(i)}, i = 1, 2, 3$, where $D^{(1)}$ and $D^{(3)}$ are constant-depth subdomains corresponding to h_1 and it is assumed that $h_1 > h_3$. The same decomposition is also used for the free-surface and the bottom boundaries. Finally, the vertical interfaces $\partial D_I^{(12)}$ and $\partial D_I^{(23)}$ separate the three subdomains of the vertical strip.

In this work the scattering problem of monochromatic, obliquely incident plane waves is considered, propagating with direction θ_1 with respect to the bottom contours in the region of incidence, under the effects of variable bathymetry and a horizontally non-homogeneous cross current $U(x)$, existing in $x > \alpha$; see Fig.1.

The flow associated with the cross current is parallel to the bottom contours and is described by the (given) continuous function $U(x)$. In the intermediate region, we assume an arbitrary current structure $U(x)$. Outside this region, the current is assumed to be uniform (or simply zero), i.e.,

$$U(x) = 0, \ x \leq a \text{ and } U(x) = U_3, \ x \geq b. \tag{1}$$

Assuming that the current variations are very slow and the wave motion is irrotational, and restricting ourselves to linear, harmonic waves of absolute frequency ω,

periodic in the $y-$direction, the wave potential can be expressed in the form (see e.g. [5]),

$$\Phi(x,y,z;t) = \Re\left(\phi(x,y,z)\exp(-i\omega t)\right), \tag{2}$$

where

$$\phi(x,y,z) = \varphi(x,z)\exp(i(qy)). \tag{3}$$

In Eqs.(2),(3), $\phi(x,y,z)$ is the complex wave potential and $\varphi(x,z)$ the reduced one on the vertical plane, q is the periodicity constant along the y-direction, and i is the imaginary unit.

The problem is governed by the Laplace equation on $\phi(x,y,z)$ or the modified Helm-holtz equation on $\varphi(x,z)$, the free-surface condition and the no-entrance condition at the bottom surface,

$$\frac{\partial^2\varphi}{\partial^2 x} + \frac{\partial^2\varphi}{\partial^2 z} - q^2\varphi = 0, \tag{4a}$$

$$\frac{\partial\varphi}{\partial z} - \mu(x)\varphi = 0, \qquad z = 0, \tag{4b}$$

$$\frac{\partial\varphi}{\partial z} + \frac{dh}{dx}\frac{\partial\varphi}{\partial x} = 0, \qquad z = -h(x). \tag{4c}$$

where $\mu(x) = \sigma^2/g$ is the frequency parameter, $\sigma = \sigma(x) = \omega - qU(x)$ is the corresponding local intrinsic frequency and g is the acceleration due to gravity.

The problem of water-wave scattering by current, with the effects of variable bathyme-try, can be formulated as a transmission problem in the bounded subdomain $D^{(2)}$, with the aid of the following general representations of the wave potential $\varphi(x,z)$ in the semi-infinite strips $D^{(1)}$ and $D^{(3)}$ (see, e.g., [3], [4]):

$$\varphi^{(1)}(x,z) = \left(A_0 exp\left(ik_0^{(1)}x\right) + A_R exp\left(-ik_0^{(1)}x\right)\right)Z_0^{(1)}(z) + \\ + \sum_{n=1}^{\infty} C_n^{(1)} Z_n^{(1)}(z)\, exp\left(k_n^{(1)}(x-a)\right), \text{ in } D^{(1)}, \tag{5a}$$

$$\varphi^{(3)}(x,z) = A_T exp\left(ik_0^{(3)}x\right) Z_0^{(3)}(z) \\ + \sum_{n=1}^{\infty} C_n^{(3)} Z_n^{(3)}(z)\, exp\left(k_n^{(3)}(b-x)\right), \text{ in } D^{(3)}. \tag{5b}$$

The terms $\left(A_0\exp\left(ik_0^{(1)}x\right)+A_R\exp\left(-ik_0^{(1)}x\right)\right)Z_0^{(1)}(z)$ and $A_T\exp\left(ik_0^{(3)}x\right)Z_0^{(3)}(z)$ in the series (5a), (5b) are the *propagating modes*, while the remaining ones ($n = 1, 2, \ldots$) are the *evanescent modes*. Specific forms of the coefficients $k_0^{(i)}$, $k_n^{(i)}$ and functions $\left\{Z_n^{(i)}(z), n = 0, 1, 2, \ldots\right\}$ can be found in [1].

Since the current is zero in $D^{(1)}$, $\sigma = \omega$, and thus, $q = \kappa_0^{(1)}\sin\theta_1$. The direction of the transmitted wave in $D^{(3)}$ is then given by

$$\theta_3 = \sin^{-1}\left(\kappa_0^{(1)}\sin\theta_1/\kappa_0^{(3)}\right). \tag{6}$$

where $\kappa_0^{(i)}$, $i = 1,3$ are the wavenumbers corresponding to the two half-strips of constant depth h_i, $i = 1,3$ obtained as the roots of the dispersion relations for the local intrinsic frequencies, see details in [1]. Given the representations Eqs. (5a), (5b), the problem can be re-formulated as a transmission boundary value problem in the bounded subdomain $D^{(2)}$, consisting of the following equations, boundary and matching conditions:

$$\nabla^2\varphi^{(2)} - q^2\varphi^{(2)} = 0, \qquad (x,z) \in D^{(2)}, \tag{7a}$$

$$\frac{\partial\varphi^{(2)}}{\partial\, n^{(2)}} - \mu\,(x)\,\varphi^{(2)} = 0, \qquad (x,z) \in \partial D_F^{(2)}, \tag{7b}$$

$$\frac{\partial\varphi^{(2)}}{\partial n^{(2)}} = 0, \qquad (x,z) \in \partial D_\Pi^{(2)}, \tag{7c}$$

$$\varphi^{(2)} = \varphi^{(1)}, \quad \frac{\partial\varphi^{(2)}}{\partial n^{(2)}} = -\frac{\partial\varphi^{(1)}}{\partial\, n^{(1)}}, \qquad (x,z) \in \partial D_I^{(12)}, \tag{7d}$$

$$\varphi^{(2)} = \varphi^{(3)}, \quad \frac{\partial\varphi^{(2)}}{\partial n^{(2)}} = -\frac{\partial\varphi^{(3)}}{\partial n^{(3)}}, \qquad (x,z) \in \partial\, D_I^{(23)}, \tag{7e}$$

where $n^{(i)} = \left(n_x^{(i)}, n_z^{(i)}\right)$ denotes the unit normal vector to the boundary $\partial D^{(i)}$ directed to the exterior of $D^{(i)}$, $i = 1,2,3$.

3. The coupled-mode system of equations

Following the procedure presented in [1], the problem on $\varphi^{(2)}(x,z)$ is treated using the following *enhanced local-mode representation* of the wave field (in the variable bathymetry region $D^{(2)}$ containing also the current variations):

$$\varphi^{(2)}\,(x,z) = \varphi_{-1}\,(x)\,Z_{-1}\,(z;x) + \varphi_0\,(x)\,Z_0\,(z;x) + \sum_{n=1}^{\infty}\varphi_n\,(x) Z_n\,(z;x) \tag{8}$$

In Eq.8 the term $\varphi_0\,(x)\,Z_0\,(z;x)$ is the *propagating mode* of the wave field and the remaining terms $\varphi_n\,(x)\,Z_n\,(z;x)$, $n = 1,2,\ldots$ are the *evanescent modes*. The additional term $\varphi_{-1}\,(x)\,Z_{-1}\,(z;x)$ is a correction term called the *sloping-bottom mode*, which accounts for the bottom boundary condition on the sloping parts of the bottom and which identically vanishes on the horizontal parts of the bottom. The function $Z_n\,(z;x)$ represents the vertical structure of the n-th mode. The function $\varphi_n\,(x)$ describes the horizontal pattern of the n-th mode and is called the *complex amplitude* of the n-th mode (modal amplitude). The functions $Z_n\,(z;x)$, $n = 0,1,2...$, appearing in Eq. 8 are obtained as the eigenfunctions of local vertical *Sturm-Liouville* problems, and are given in [1]. A specific convenient form of the function $Z_{-1}\,(z;x)$ is given by

$$Z_{-1}\,(z;x) = h\,(x)\left[\left(\frac{z}{h\,(x)}\right)^3 + \left(\frac{z}{h\,(x)}\right)^2\right], \tag{9}$$

and all numerical results presented in this work are based on the above choice for $Z_{-1}(z;x)$. However, other choices are also possible. The main effect of the additional sloping-bottom mode $\varphi_{-1}(x)\, Z_{-1}(z;x)$ is that it makes the series (8) compatible with the bottom boundary condition (7c) on the sloping parts of the bottom surface.

By using the local-mode series representation (8) in conjunction with an equivalent variational formulation of the transmission problem, and by following exactly the same procedure as in [11], the following coupled-mode system is obtained:

$$\sum_{n=-1}^{\infty} a_{mn}(x)\,\varphi_n''(x) + b_{mn}(x)\,\varphi_n'(x) + \left(c_{mn}(x) - a_{mn}(x)\,q^2\right)\varphi_n(x) = 0,$$
$$a < x < b, \qquad m = -1, 0, 1, ... \tag{10}$$

where a prime denotes differentiation with respect to x. The expressions of the coefficients a_{mn}, b_{mn}, c_{mn} of the system (10) are the same as given in Table 1 of [11]. The system (10) is supplemented by the following decoupled end-conditions

$$\varphi_{-1}(a) = \varphi_{-1}'(a) = 0, \qquad \varphi_{-1}(b) = \varphi_{-1}'(b) = 0, \tag{11a}$$
$$\varphi_0'(a) + ik_0^{(1)}\varphi_0(a) = 2\,i\,k_0^{(1)}\exp\left(i\,k_0^{(1)}a\right), \qquad \varphi_0'(b) - ik_0^{(3)}\varphi_0(b) = 0, \tag{11b}$$
$$\varphi_n'(a) - k_n^{(1)}\varphi_n(a) = 0, \qquad \varphi_n'(b) + k_n^{(3)}\varphi_n(b) = 0, \tag{11c}$$

where $n = 1, 2, \ldots$ and the coefficients $k_n^{(1)}$, $k_n^{(3)}$, can be found in [1]. Furthermore, the reflection and transmission coefficients (A_R, A_T) appearing in Eqs.(5a), (5b) are obtained from the solution of the coupled-mode system as follows:

$$A_R = \left(\varphi_0(a) - \exp\left(i\,k_0^{(1)}a\right)\right)\exp\left(i\,k_0^{(1)}a\right),\ A_T = \varphi_0(b)\exp\left(-i\,k_0^{(3)}b\right). \tag{12}$$

An important feature of the solution of the present scattering problem by means of the representation 8, is that it exhibits an improved rate of decay of the modal amplitudes $|\varphi_n(x)|$ of the order $O\left(n^{-4}\right)$, see [11], Sec. 4. Thus, a small number of modes suffices to obtain a convergent solution to $\varphi(x,z)$, even for large bottom slopes.

4. The Wavelet-Galerkin technique

The construction of the discrete system is obtained by truncating the local-mode representation (8) to a finite total number of modes, retaining only a small number of evanescent modes.

A Wavelet-Galerkin method is used for the numerical solution of the truncated coupled mode system of equations (10). The horizontal modal amplitudes of the coupled modes may be represented with the help of wavelet series as follows

$$\varphi_n(x) = \sum_{j=J_0}^{J_{\max}} \sum_{i=I(a)}^{I(b)} d_{ij}^n \psi_{ij}(x) \tag{13}$$

where J_0, $J_{\max}$ are integers, indicating the lowest and highest levels of resolution respectively (wavelet scales), and $I(a)$, $I(b)$ are integers indicating the limits of the position of the wavelet functions in space. For simplicity, we avoid presenting the scaling functions of the coarsest level of resolution which are considered to be incorporated in the above double sum. The support of the expansion (13) $[-p+1/2^{J_{max}}+a, p-1/2^{J_{max}}+b]$, where p is the number wavelet filter coefficients used for the numerical implementation of the wavelet transform. Introducing this representation in the coupled-mode system of equations (10), the final system assumes the form,

$$\sum_n \mathcal{D}_n^m \varphi_n(x) = \sum_{n=0}^{\infty} a_{mn}(x) \sum_{j=J_0}^{J_{\max}} \sum_{i=I(a)}^{I(b)} d_{ij}^n \psi_{ij}''(x) + b_{mn}(x) \sum_{j=J_0}^{J_{\max}} \sum_{i=I(a)}^{I(b)} d_{ij}^n \psi_{ij}'(x) +$$

$$+ \left(c_{mn}(x) - a_{mn} q^2\right) \sum_{j=J_0}^{J_{\max}} \sum_{i=I(a)}^{I(b)} d_{ij}^n \psi_{ij}(x) = 0, \quad m = 0, 1, 2, \ldots, \quad a \le x \le b, \tag{14}$$

where $\mathcal{D}_n^m = a_{mn}(x) \frac{\partial^2}{\partial x^2} \bullet + b_{mn}(x) \frac{\partial}{\partial x} \bullet + \left(c_{mn}(x) - a_{mn}(x) q^2\right) \bullet$. Following the Galerkin technique, we project these equations to the space generated by the functions $\{\psi_{ij}\}$ and, retaining a small number of modes $N_{\max}$, we obtain the following set of equations

$$\left\langle \sum_n \mathcal{D}_n^m \varphi_n(x), \psi_{kl}(x) \right\rangle = \sum_n \left\{ d_{ij}^n \left\langle \sum_{j=J_0}^{J_{\max}} \sum_{i=I(a)}^{I(b)} D_n^m \psi_{ij}(x), \psi_{kl}(x) \right\rangle \right\} = 0,$$

$$k = J_0, J_0+1, ..., J_{\max}, \quad l = I(a), I(a)+1, ..., I(b), \quad m = 0, 1, ..., N_{\max}, \tag{15}$$

where $\langle f(x), g(x) \rangle = \int_{-\infty}^{\infty} f(x) \bar{g}(x) dx$ and overbar denotes the complex conjugate. Hence, we obtain a system of equations, for the wavelet coefficients d_{ij}^n. The inner products,

$$\langle \psi_{ij}(x), \psi_{kl}(x) \rangle = \Gamma_{ij}^{0,kl}, \ \langle \psi_{ij}'(x), \psi_{kl}(x) \rangle = \Gamma_{ij}^{1,kl}, \ \langle \psi_{ij}''(x), \psi_{kl}(x) \rangle = \Gamma_{ij}^{2,kl}, \tag{16}$$

are called wavelet *connection coefficients* and are numerically computed, see e.g. [12].

An intrinsic problem of the wavelet-Galerkin technique (regardless of the dimensionality of the problem) is the imposition of boundary conditions. Wavelets are functions of compact support and, in order to represent any function at a specific point of the domain, a number of neighbouring wavelets, having support that includes this point, are needed. This poses a problem for the points that are close to the boundaries of the domain. In order to tackle this problem, a technique first implemented by Lu *et al.* [13], is used. According to this technique, the real domain of the solution is extended to match the support of the representation (fictitious domain). The boundary conditions are imposed on the real boundaries a,b, thus the solution

satisfies both the governing equation and the real boundary conditions. For example, the boundary condition

$$\varphi_0'(a) + ik_0^{(1)}\varphi_0(a) = 2ik_0^{(1)}\exp\left(ik_0^{(1)}a\right), \tag{17}$$

assumes the form,

$$\sum_{j=J_0}^{J_{\max}}\sum_{i=I(a)}^{I(b)} d_{ij}^n\ \psi_{ij}'(x) + ik_0^{(1)}\sum_{j=J_0}^{J_{\max}}\sum_{i=I(a)}^{I(b)} d_{ij}^n\psi_{ij}(x) = 2ik_0^{(1)}\exp\left(ik_0^{(1)}a\right),\ x=a, \tag{18}$$

where $\psi_{ij}'(x) = \sum_{kl}\Gamma_{ij}^{1,kl}\psi_{kl}(x)$, and after using the Galerkin technique, it is properly placed in the system of equations, see [13]. The part of the solution that lies outside the real domain is ignored.

Using wavelets of increasing smoothness, e.g. Daubechies wavelets, the number of grid points per wavelength required for numerically stable computation decreases (8 points for Daubechies-9, 3 points for Daubechies-20), see ([9]). Thus, less computational points are needed for accurate numerical results, leading to a smaller system of equations. On the other hand, for higher smoothness wavelets, the length of the corresponding wavelet filters and, consequently, the number of connection coefficients, are increased. Thus, the final matrix of the linear system, produced by using smoother wavelets, is more dense (quasi-sparse).

For the solution of the linear system (15), after imposing the boundary conditions, an algorithm that takes full advantage of the wavelet representation, and was first presented in ([10], is used. This algorithm approximates the unknown solution $\varphi_n(x)$ by an arbitrary linear combination of N wavelets (N-term approximation), which would be obtained by keeping the N largest wavelet coefficients of the solution. An adaptive iterative solution scheme provides the final solution (proof of the convergence of the scheme can be found in ([10]). At each step of the process, the unknown coefficients of the solution are recalculated in a way that their number remains minimum without a significant loss of accuracy. The algorithm also takes advantage of wavelet compression properties to perform fast multiplication of quasi-sparse matrices with vectors.

5. Numerical results

The combined effects of variable bathymetry and shear current on the form of the wave field is examined in the case of a smooth but steep under water shoal with an over-imposed sandbar at the shallow end. The depth function is given by,

$$\begin{aligned} h(x) = {} & \hat{h} - \frac{h_1 - h_3}{2}\tanh\left(2.5\pi\left(\frac{x-a}{b-a} - \frac{1}{2}\right)\right) - \hat{h}\exp\left(\frac{-(x-x_1)^2}{\ell^2}\right) \\ & - 0.8\hat{h}\exp\left(\frac{-(x-x_2)^2}{\ell^2}\right),\ a = 0 < x < b = 40m \end{aligned} \tag{19}$$

where $\hat{h} = \frac{h_1+h_3}{2}$, $\ell = \frac{b-a}{16}$, $x_1 = a + \frac{b-a}{2}$, $x_2 = a + \frac{2(b-a)}{3}$, $h_1 = 20m$, $h_3 = 5m$. This bottom profile has mean slope $s_{mean} = 0.63$ and maximum slope $s_{max} = 3.02$ (see Fig. 2). An opposing current is considered, given by,

$$U(x) = \frac{c_1}{4} + \frac{c_1}{4} \tanh\left(3\pi\left(\frac{x-a}{b-a} - \frac{1}{2}\right)\right), \; a = 0 < x < b = 40m \tag{20}$$

where c_1 is the phase speed of the incident waves in $D^{(1)}$. The period and the direction of the incident wave is taken to be $T = 6$sec and $\theta_1 = 30^o$ respectively and thus $c_1 = 9.175$m/sec. The effect of the opposing current can be seen in Fig.2a on both vertical ($y = 0$) and horizontal ($z = 0$) plane where the real part of the wave filed is plotted. In this case the reflection and transmission coefficients are $|A_R| = 0.198$, $|A_T| = 0.686$ showing a significant reflection effect due to the presence of the current. The later result can be compared to a similar one for the case without the effect of the opposing current, presented in Fig.2b. In this case the reflection and transmission coefficients are $|A_R| = 0.093$, $|A_T| = 0.935$ showing only the effect of the abrupt shoaling. In the modal series expansion, a small number of modes (5 terms) have been retained, which has been proved enough for numerical convergence, even for such large gradients of the depth function. In all cases (see upper images in Fig.2), the equipotential lines intersect the bottom surface perpendicularly, which is evidence of satisfaction of the bottom boundary condition, both on the horizontal and on the sloping parts of the bottom.

Daubechies third wavelet was used for the representation of the modal amplitudes, for the above numerical results. An initial number of 512 wavelet coefficients is used for the representation of each modal amplitude, corresponding to a total of $5 \times 512 = 2560$ unknown coefficients. The compressed form of the representation is acquired after applying the previously mentioned algorithm for a total of 600 wavelet coefficients and is practically the same as its uncompressed form. The relative error induced by the compression is of order 10^{-7}, in the energy norm. A small percentage of the initial coefficients allows us to efficiently represent the solution.

In Fig.3 a typical structure of the modal amplitudes of the propagating, the second evanescent and the sloping bottom mode is presented. It is clear that over regions of abrupt changes of the bathymetry and the current strength, the modal amplitudes of the evanescent modes consist of a variety of scales localised in space. The same behaviour appears also in the structure of the sloping bottom mode, which however vanishes by definition in areas of constant depth. Wavelets can "recognise" these regions consisting of small scales or sharp transitions. Wavelets of the higher scales (smaller support and higher frequency content) are strongly correlated with such regions of a function, leading to large coefficients in the vicinity of these regions, whereas in regions consisting of large scales (low frequencies) higher scale wavelets coefficients are almost zeros and can be ignored. This becomes obvious in the above Fig.3, where stars correspond to wavelet coefficients of various scales.

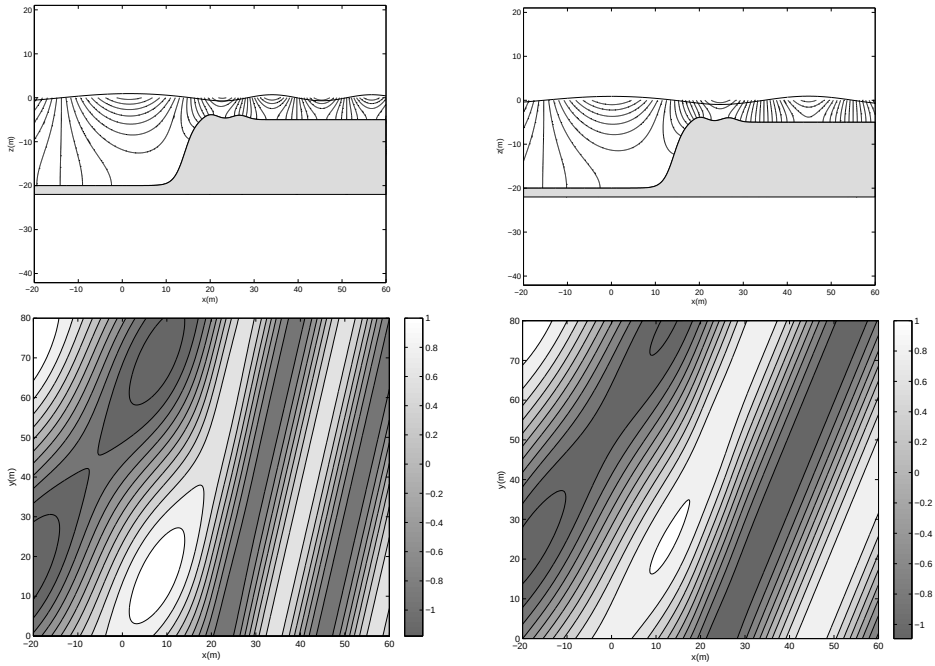

(a) Wave field under the effect of an opposing shear current.

(b) Wave field with no current present.

Figure 2: Calculated wave field (real part) in the case of an obliquely incident monochromatic wave, with direction of 30^o, over a smooth and abrupt shoaling with the presence of sandbars in the shallow area. The fulfilment of the bottom boundary condition can be verified by the verticality of the equipotential lines on the bottom surface.

6. Concluding remarks

A Wavelet-Galerkin technique has been developed for the wave-current-seabed interaction problem, with application to wave scattering by steady currents in variable bathymetry regions. Based on an appropriate variational principle, in conjunction with a rapidly convergent local-mode series expansion of the wave field in a finite subregion, containing the current variation and the bottom irregularity, the problem is reformulated as a coupled-mode system; see also [1]. This system can be considered as a generalisation of the one derived in [11] for the propagation of waves in variable bathymetry regions without the effect of current. The key features of the present method is the introduction of an additional mode, completely describing the influence of the bottom slope, the wavelet series representation of the modal amplitudes and the efficient solution of the problem taking advantage of wavelet properties.

The main advantage of using wavelets in comparison to other solution schemes,

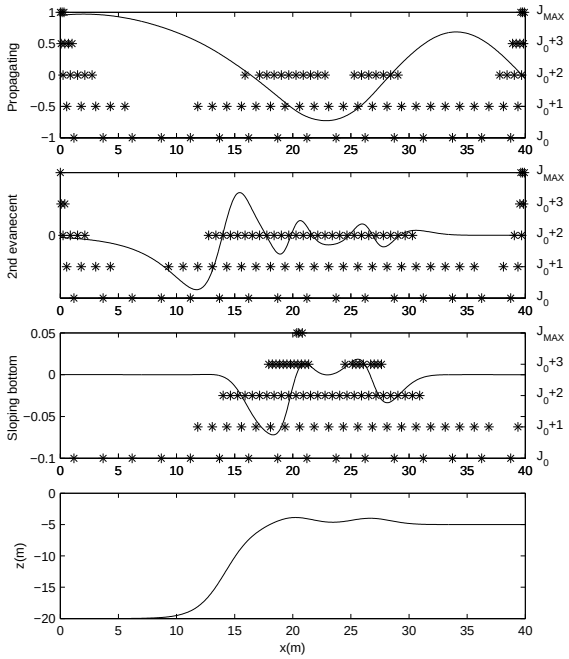

Figure 3: The spatial distribution of the wavelet coefficients of the modal amplitudes, for each scale $J_0, J_0 + 1, ., J_{max}$. The real part of modal amplitudes is denoted using continuous line.

e.g. finite differences, is their intrinsic ability to resolve a variety of spatial scales that are known to be present in the solution. Moreover, high compression rates achieved by wavelets, lead to an accurate and efficient recursive solution of the final system of equations.

The structure of the present model facilitates its extension to various directions as, e.g., to three-dimensional problems and to more complex wave-current systems, including the effects of lateral discontinuities (e.g. vertical vortex sheets), the effects of more general vertical current profiles with cross-jet component, and the effects of weak nonlinearity.

Acknowledgements

The present work has been supported by the Operational Program for Educational and Vocational Training II (EPEAEK II) and particularly the PYTHAGORAS II project. The project is co-funded by the European Social Fund (75%) and National Resources (25%).

References

1. K.A. Belibassakis and G.A. Athanassoulis. A coupled-mode technique for wave-current interaction in variable bathymetry regions. In Chung J.S. et al, editor, *Proc. of 14th Intern. Offshore and Polar Conference and Exhibition, ISOPE, Toulon, France*. ISOPE, 2004.
2. K.A Belibassakis. Propagation of water waves through shearing currents in general bathymetry. In Soares C.G et al, editor, *Proc. of 14th Intern. Congress of Int. Maritime Association of the Mediterranean, IMAM, Lisbon, Portugal*. IMAM, 2005.
3. J. Smith. On surface gravity waves crossing weak current jets. *Journal of Fluid Mechanics*, 134:277–299, 1983.
4. J. Smith. On surface waves crossing a step with horizontal shear. *Journal of Fluid Mechanics*, 175:395–412, 1987.
5. C.C. Mei. *The applied dynamics of ocean surface wave*. John Wiley & Sons, 1983, 2nd Reprint, 1994, World Scientific.
6. D. Faulkner. Rogue waves defining their characteristics for marine design. In M. Olagnon and G.Athanassoulis, editors, *Proc. Rogue Waves, Brest, France*, pages 3–18. Ifremer, 2000.
7. K.B. Dysthe. modelling a rogue wave speculations or a realistic possibility. In M. Olagnon and G.Athanassoulis, editors, *Proc. Rogue Waves, Brest, France*, pages 255–264. Ifremer, 2000.
8. I.V. Lavrenov and A.V. Porubov. Three reasons for freak wave generation in the non-uniform current. *European Journal of Mechanics B/Fluids*, 25:574–585, 2006.
9. G. Strang and T. Nguyen. *Wavelets and Filter Banks*. Wellesley-Cambridge Press, 1996.
10. A. Cohen, W. Dahmen, and R. Devore. Adaptive wavelet methods for elliptic operator equations: Convergence rates. *Mathematics of Computation*, 40(233):27–75, 2000.
11. G.A. Athanassoulis and K.A. Belibassakis. A consistent coupled-mode theory for the propagation of small-amplitude water waves over variable bathymetry regions. *J. Fluid. Mech.*, 389:275–301, 1999.
12. A. Latto, H.L. Resnikoff, and E. Tenebaum. The evaluation of connection coefficients of the compactly supported wavelets. In Y. Maday, editor, *Proc. French-USA Workshop on Wavelets and Turbulence,1992*. Prinston University, Springer, NY, 1992.
13. D. Lu, T. Ohyoshi, and L. Zhu. Treatment of boundary conditions in the application of wavelet-galerkin method an sh wave problem. *International Journal of the Society of Materials Engineering For Resources*, 5(1):15–25, 1997.

◇ Th.P. Gerostathis
School of Naval Architecture and
Marine Engineering
National Technical University of Athens
GR-157 80 Athens, GREECE
tgero@central.ntua.gr

◇ K.S. Politis
School of Naval Architecture and
Marine Engineering
National Technical University of Athens
GR-157 80 Athens, GREECE
politesc@central.ntua.gr

◇ K.A. Belibassakis
Department of Naval Architecture
Technological Educational Institute of Athens
GR-122 10 Athens, GREECE
kbel@teiath.gr

◇ G.A. Athanassoulis
School of Naval Architecture and
Marine Engineering
National Technical University of Athens
GR-157 80 Athens, GREECE
mathan@central.ntua.gr